

Proceedings of the Research Institute of Atmospheric,
Nagoya University, vol. 32(1985)

TECHNICAL NOTE

GROUND-BASED RECEPTION OF THE WHISTLER MODE DECCA SIGNALS

Akira IWAI, Yasuo KATOH, Masanori NISHINO, Toshimi OKADA,
Masashi HAYAKAWA and Yoshihito TANAKA

Abstract

Measurements of the whistler-mode magnetospheric waves of the Decca signal (85.725 kHz, CW, 1.2 kW) transmitted from Biei ($L = 1.54$), Japan were carried out from July 10 to September 7, 1984 at Birdsville, Australia, the geomagnetic conjugate point of the transmitter. We describe the measurement system of the whistler-mode waves, which were identified by detecting the polarization and Doppler-shifted components. Several examples of the observed results are reported.

1. Introduction

An active experiment by means of transmission of VLF signals is being conducted near the plasmopause between the conjugate stations : Siple ($L=4$) and Roberval, which has yielded interesting phenomena on non-linear whistler interaction (Helliwell and Katsufurakis, 1978).

It is well known that abundant energetic particles are present at those L shells for wave-particle interactions. While, the L value of our Moshiri Observatory is 1.59, being situated at the outer edge of the inner zone radiation belt, and the wave-particle interactions there are not well understood. We are exploring the feasibility of an active experiment on wave-particle interactions at $L = 1.6 (f_{Heq} \sim 220 \text{ kHz})$ in which we will transmit the high power LF ($\sim 100 \text{ kHz}$) signals from Moshiri (Hayakawa et al., 1983). Field-aligned (ducted) propagation is essential for wave-particle interactions. LF waves in ducted mode which are not totally internally reflected can escape from the lower ionosphere, but compared with VLF waves, the LF waves are heavily attenuated when penetrating through the lower ionosphere, except in a small directional range about the geomagnetic field. In addition to the ionospheric propagation effect, the locality due to the magnetospheric propagation effect is strong at LF, so that the whistler-mode LF waves could be detectable in a localized region around the conjugate point of the transmitter. As a step toward developing an active experiment, we carried out measurements of the whistler-mode waves of the Decca signal transmitted from Biei (near Moshiri) at its conjugate point, Birdsville in Queensland, Australia in 1983 and 1984. In the preliminary campaign of the first year (August 11-28, 1983), the subionospheric waves propagated from the transmitter in the earth-ionosphere waveguide were recorded at night, the intensities of which amounted to be $\sim 1 \mu\text{V/m}$, but the whistler-mode signals were not identified, probably due to impulses of atmospherics disturbing a detection system by means of the lock-in-amplifiers. In this paper, we introduce an improved measurement system to detect the whistler-mode Decca signals adopted for the second year's campaign (July 10 - September 7, 1984) and present some of the obtained results.

2. General Design

We designed the measurement system, according to the following basic considerations : (1) detection of signals with intensities as low as $\geq 0.1 \mu\text{V/m}$, referring to the received intensities ($\sim 1 \mu\text{V/m}$) of the subionospheric Decca signals of 85.725 kHz at night during the campaign of 1983, and (2) reduction of interferences from atmospherics and Decca signals of 85.635 kHz from Dampier, Australia, which is only 90 Hz apart from our target Decca signal of 85.725 kHz, and (3) distinction

of the whistler-mode from the subionospheric mode, based on detecting the wave polarization and the Doppler shift of the receiving frequency.

For the campaign of 1983, the output from the preamplifier was fed to a bandpass filter with the bandwidth of 560 Hz centred at 85.725 kHz. Such rather wide-banded output signals including atmospheric and other Decca signals, saturated, from time to time, the lock-in-amplifiers. Moreover, the time constant for locking the faint CW against atmospheric impulses was set at a large value of 10 sec., corresponding to a bandwidth $B = 1/(2T) = 0.05$ Hz. As the result, the whistler-mode Decca signals might deviate out of the tuned frequency range, due to the Doppler shift. Hence, our revised system for 1984 adopts crystal filters with the bandwidth of 20 Hz, simultaneous recording of the centred frequency component and the frequency shifted ones at an interval of ± 0.5 Hz, and an integration of rectified signal of each frequency component to depress interferences of atmospheric.

The phase variations of the subionospheric waves at LF and VLF measured by means of a phase tracking equipment reach ~ 720 degrees (2 cycles) or more at sunrise and sunset during a short period such as ~ 30 minutes (Chilton et al., 1963; Doherty, 1964). The frequency shift corresponding to the phase shift may be estimated to be of the order of 10^{-3} Hz on the average, which is smaller by two orders than the frequency shift of the whistler-mode NLK signals at 18.6 kHz with a maximum of ~ 14 PPM (McNeill and Andrews, 1975). The Doppler shift (Δf) of the whistler-mode waves is expressed by

$$\Delta f = -\frac{f}{c} \frac{\partial}{\partial t} \int_{\text{path}} \mu \, dS \propto \sqrt{f}$$

, where f is the wave frequency, c the light speed and μ the refractive index. So, we may estimate analogically the maximum Doppler shift of about 0.6 Hz at 85.725 kHz from the value of Doppler shift at 18.6 kHz.

3. Measurement System

Fig.1 illustrates the block diagram of the measurement system which is composed of the antennas, preamplifiers, main amplifiers and data recording equipments. Fig.2 shows the level diagram of the measurement system. Fig.3 presents a photograph of the measurement apparatuses set up in the observation room which is about 50 meters apart from the antenna site.

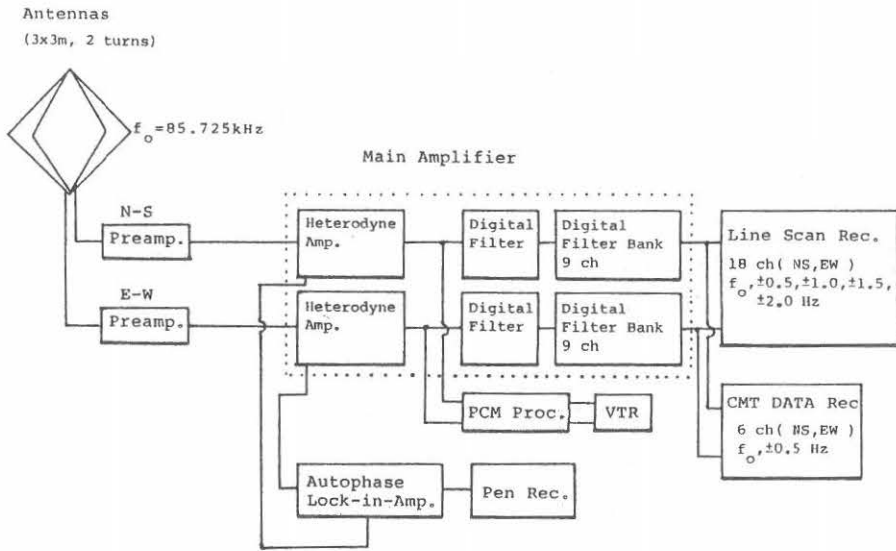


Fig.1 Block diagram of the measurement system.

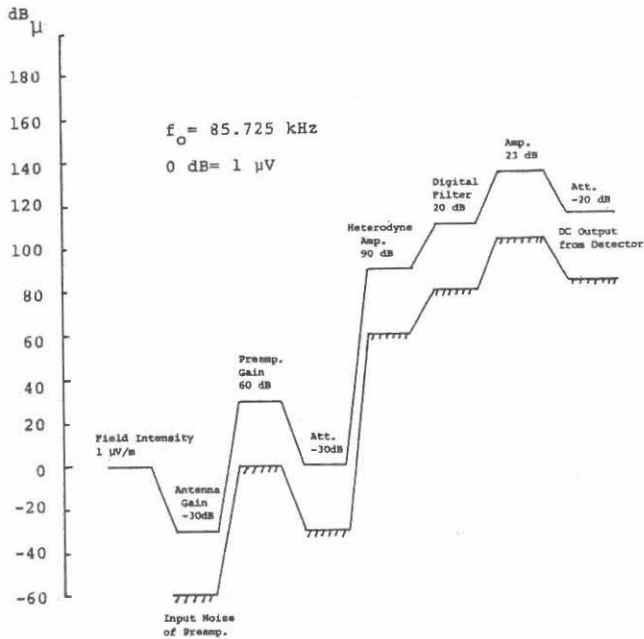


Fig.2 Level diagram of the measurement equipments in dBμ (0 dB= 1 μV) at 85.725 kHz with reference to the input noise voltage of the preamplifier (- 60 dBμ) within the bandwidth of 0.5 Hz, and the average field intensity (1 μV/m) of received Decca signals.

3-1 Antennas

Constructed were the crossed loop diamond-shaped antennas (3 x 3 m, 2 turns, effective height of 3.2 cm at 85.725 kHz) with the planes directed in the geomagnetic NS and EW directions('NS' and 'EW' antennas). The input noise voltage of the preamplifier is 10^{-9} v within the bandwidth of 0.5 Hz, so that the minimum detection level of signals is expected to be $\approx 0.03 \mu\text{V/m}$. Fig.4 shows a photograph of the crossed loop antennas.

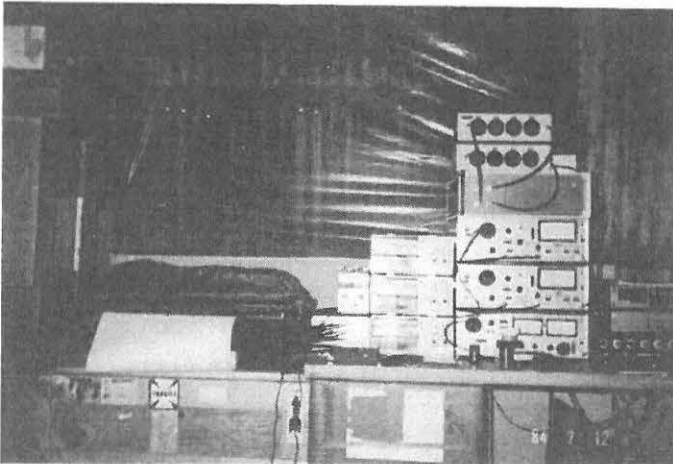


Fig.3 Photo of the measurement apparatuses.

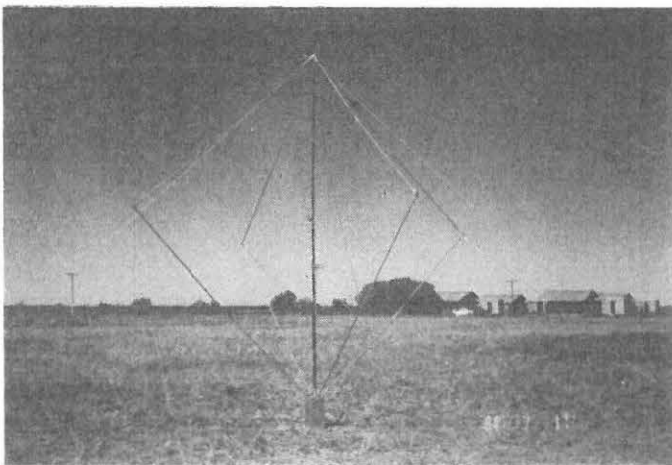


Fig.4 Photo of the crossed loop antennas.

3-2 Main Amplifier

The NS and EW outputs from the preamplifiers installed just below the antennas are fed to the main amplifier consisting of a pair of heterodyne amplifiers, digital filters and digital filter banks. Fig.5 shows the block diagram of the heterodyne amplifiers where outputs from the preamplifiers are led to crystal filters($\Delta f = \pm 10$ Hz) whose attenuation characteristics are represented in Fig.6. The NS and EW narrow-banded signals centred at 85.725 kHz are branched to an autophase lock-in-amplifier, in which the phase difference between NS and EW signals is detected, and they are also fed to the frequency converters. The narrow-banded signals are heterodyned to VLF centred at 5.725 kHz by means of the frequency converter. The frequency converted VLF signals are introduced to the digital filters, and they are also led to a VTR recorder connecting to a PCM processor('PCM recorder'), in order to record the waveforms of the NS and EW signals.

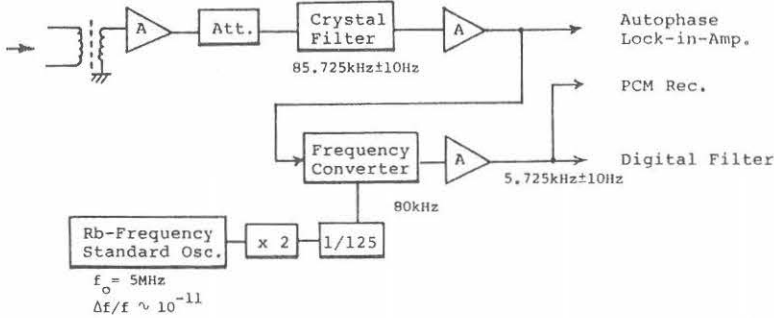


Fig.5 Block diagram of the heterodyne amplifier.

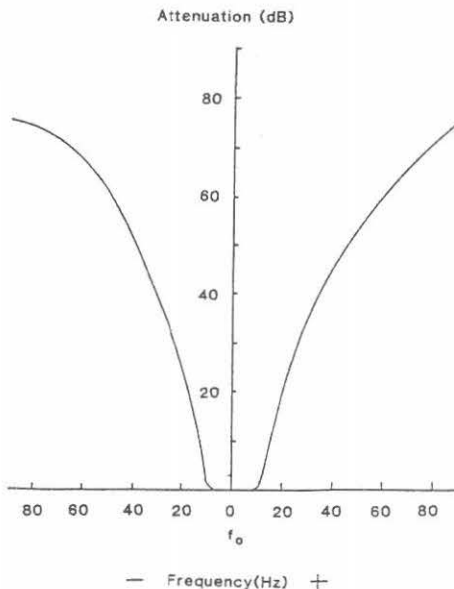


Fig.6 Attenuation characteristics of the crystal filter centred at $f_0 = 85.725$ kHz.

The VLF signals($5.725 \text{ kHz} \pm 10 \text{ Hz}$) are converted down to $715.625 \pm 10 \text{ Hz}$ through the digital filter^{*}. Then, the outputs from the digital filter are led to the digital filter bank consisting of 9 channel digital filters through which the signals are divided into 9 frequency components, corresponding to antenna input signals at 85.725 kHz , ± 0.5 , ± 1.0 , ± 1.5 and $\pm 2.0 \text{ Hz}$ with each bandwidth of 0.4 Hz ^{**}. Then, each component is rectified and integrated. The filtering characteristics of the digital filter bank are shown in Fig.7. Fig.8 presents the input-output characteristics of the main amplifier indicating the relationship between the input voltage in $\text{dB}\mu$ ($0 \text{ dB}\mu = 1 \mu\text{V}$) at 85.725 kHz and the DC output voltage of rectified signals.

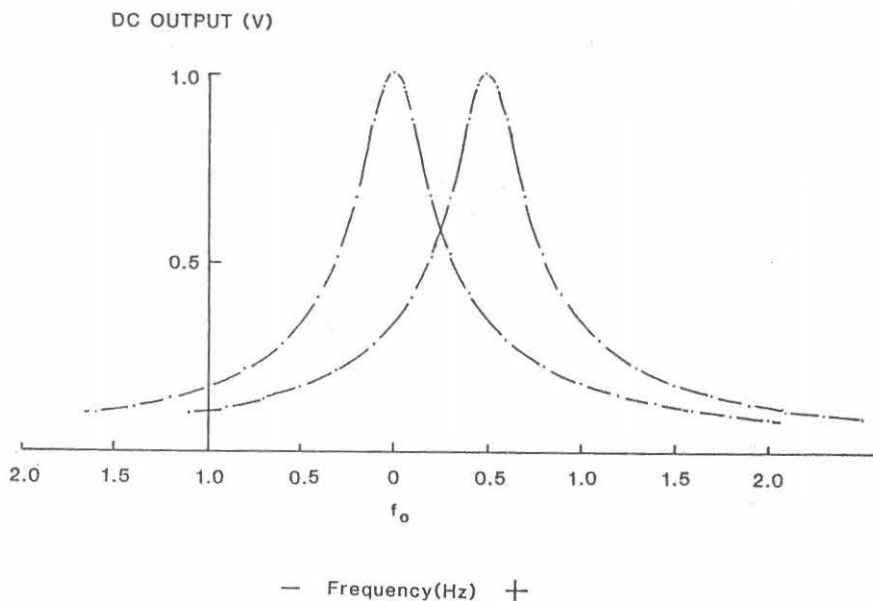


Fig.7 Filtering characteristics of the digital filter bank at 2 representative frequencies ($f_0 = 85.725 \text{ kHz}$ and $f_0 + 0.5 \text{ Hz}$), indicating the relationship between the input voltage ($7.3 \text{ dB}\mu$) to the main amplifier and the DC output voltage of the filter bank circuit.

(*), (**), Details are described in the appendix.

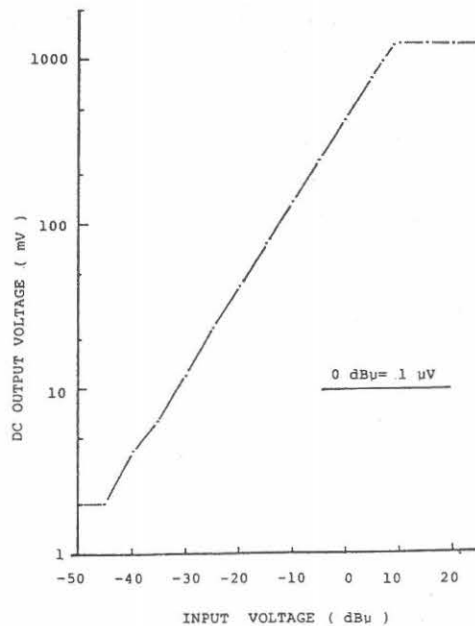


Fig.8 Input-output characteristics of the main amplifier indicating the relationship between the input voltage in dBμ and the DC output voltage.

3-3 Data Recording

The rectified signals on 18 channels(9 ch(85.725 kHz, ±0.5, ±1.0, ±1.5, and ±2.0 Hz) x 2(NS,EW)) were continuously recorded on a line scan recorder(discharging electrical energy printing at a speed of 4 sec/scan). The rectified signals on 6 channels(3 ch(85.725 kHz, ±0.5 Hz) x 2(NS,EW)) were also recorded in a CMT data recorder for further detailed analyses. Outputs from the crystal filters were led to an autophase lock-in-amplifier where the phase difference between the NS and EW signals was occasionally detected by using the NS signal itself as the external reference signal. The output signals(5.725 kHz ± 10 Hz) from the heterodyne amplifiers were fed to a PCM recorder in which the waveforms of the NS and EW signals were recorded during 1 minute every 10 minutes.

4. Observed Results

The following preliminary results are obtained, mainly based on the magnetic field intensity records on the 18 channel line scan recorder :

(1) The whistler-mode Decca signals usually appeared at sunset and sunrise, and their field intensities amounted to be $\leq 1.5 \mu\text{V/m}$ at f_0 (85.725 kHz) on the NS and EW channels.

(2) The whistler-mode signals were usually elliptically polarized and exhibited Doppler shifts of $\leq 0.5 \text{ Hz}$ and $\geq -0.5 \text{ Hz}$ at sunset and sunrise, respectively.

(3) The Decca signals were never observed during the daytime, being below the noise level. As the earth-ionosphere waveguide loss begins to decrease after sunset, the subionospheric mode of the Decca waves usually appears and is observed during the nighttime, which was found to be almost linearly polarized and to exhibit no Doppler shifts. The field intensities of the NS component reached $\sim 2 \mu\text{V/m}$ at the maximum, while the EW component was negligibly weak. The subionospheric mode is more predominant than the whistler mode at night.

(4) Associated with the geomagnetic storms, the field intensities of both NS and EW components during the nighttime increased by $\geq 20 \text{ dB}$ compared with the usual intensity level of the subionospheric mode at night. The storm-associated whistler-mode waves were elliptically polarized and Doppler-shifted. It is characteristic that the field intensities vary greatly ($\geq 20 \text{ dB}$) with a short period of the order of $\sim 2-3 \text{ sec}$.

Fig.9 shows an example of the whistler-mode Decca signals observed at sunrise, the polarization of which was detected by means of the auto-phase lock-in-amplifier and was almost circular, as shown in Fig.10. Fig.11 indicates the enhanced signals in the whistler mode appearing throughout the nighttime, associated with the geomagnetic storm of July 13-14, 1984. Fig.12 shows one example of the temporal variations of the field intensities during the geomagnetic storm of September 4-6, 1984, obtained from the data in the PCM recorder. The line scanning data indicate the average intensities for 10 sec., but during the geomagnetic storms, the field intensities on the lock-in-amplifier (the time constant, 1 sec.) and the PCM recorder seem to vary greatly ($\geq 20 \text{ dB}$) with a short period of the order of $\sim 2-3 \text{ sec}$. Such temporal variations are of essential importance in evaluating the wave-particle interactions in the magnetosphere, but they must be discussed, based on the forthcoming detailed analyses of the data in the PCM recorder.

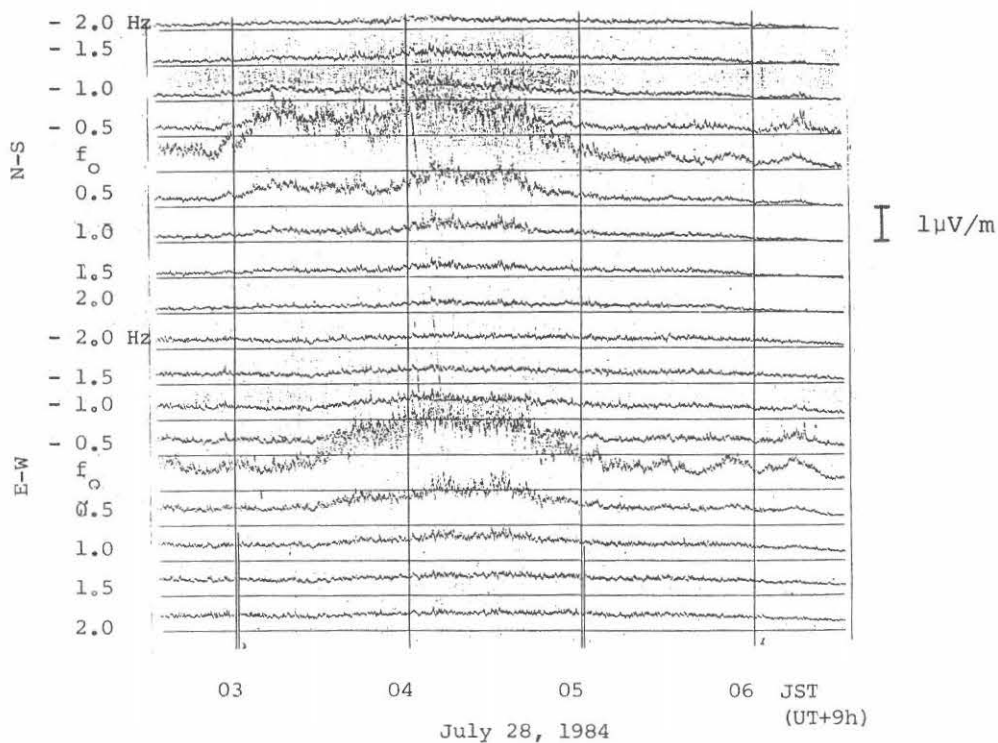


Fig.9 Magnetic field intensities on 18 ch line scan recorder for whistler mode Decca signals at sunrise on July 28, 1984 at Birdsville.

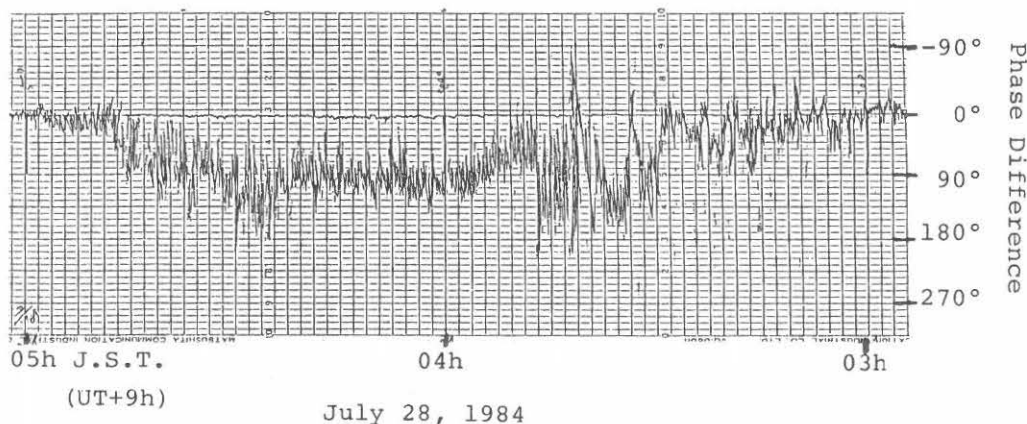


Fig.10 Phase difference detected by means of the autophase lock-in amplifier between the NS and EW signals ($85.725\text{kHz} \pm 10\text{Hz}$) for whistler mode signals at sunrise on July 28, 1984 at Birdsville, where 90° phase difference suggests almost circular polarization.

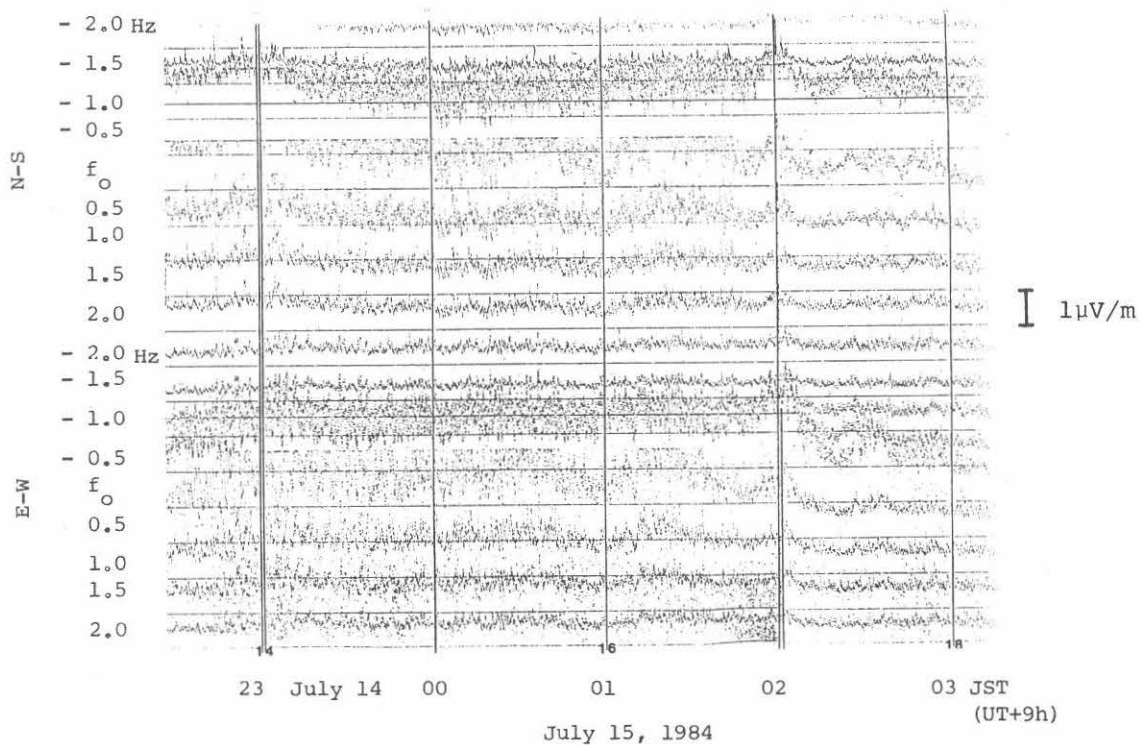


Fig.11 Enhanced signals in whistler mode on all the 18 frequency components on July 14-15, 1984 at Birdsville, associated with the geomagnetic storm of July 13-14.

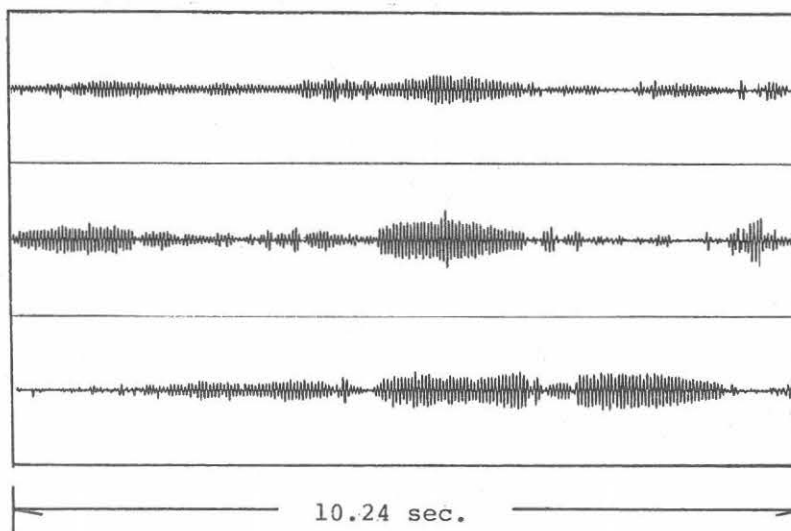


Fig.12 Temporal variations in the envelope of the amplitude of the whistler-mode NS signals recorded in the PCM recorder at 23h00m JST September 6, 1984 at Birdsville, associated with the geomagnetic storm of September 4-6.

We have investigated the locality of the whistler-mode Decca waves. The simultaneous observations using similarly performed equipments were successfully made during August 20-28, 1984 at Birdsville and at Clifton Hill which lies higher in latitude than Birdsville in the same geomagnetic meridian and is 100 km apart from there. We used the lock-in-amplifiers with the time constant of 1 sec, corresponding to the bandwidth $B = 1/(2T) = 0.5$ Hz and the pen-recording of the average intensities for ~ 5 sec on the EW channel.

Fig.13 presents an example indicating the locality of the whistler-mode Decca signals where the enhanced EW signals were observed at sunrise at Birdsville, but not at Clifton Hill. While, Fig.14 represents an example indicating the simultaneously enhanced EW signals at sunrise at the two stations, for which a few field-aligned paths (ducts) may be formed between the conjugate points of Birdsville and Biei as well as at somewhat higher latitudes.

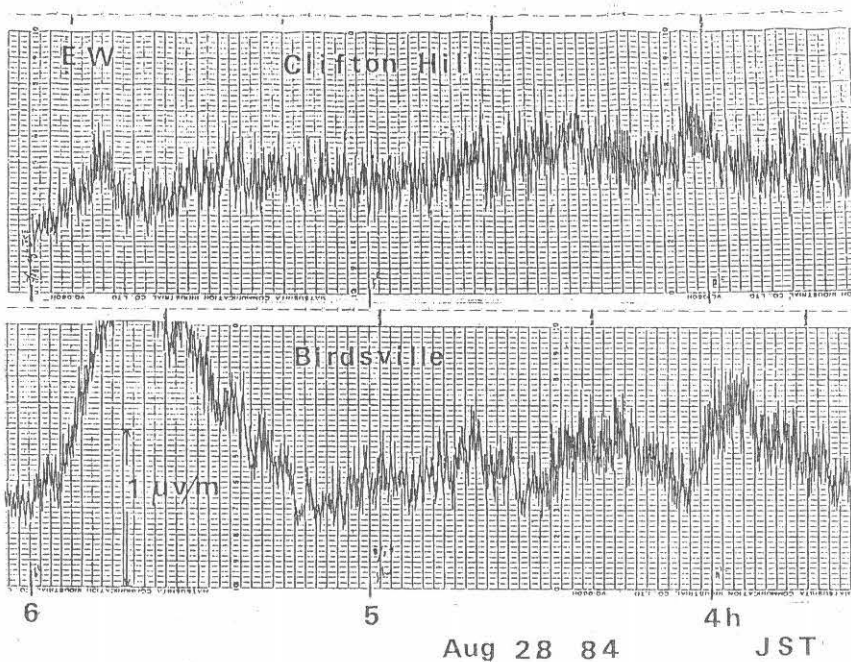


Fig.13 Enhanced EW signals observed at Birdsville but not at Clifton Hill, being ~ 100 km distant towards higher latitudes almost along the same geomagnetic meridian plane.

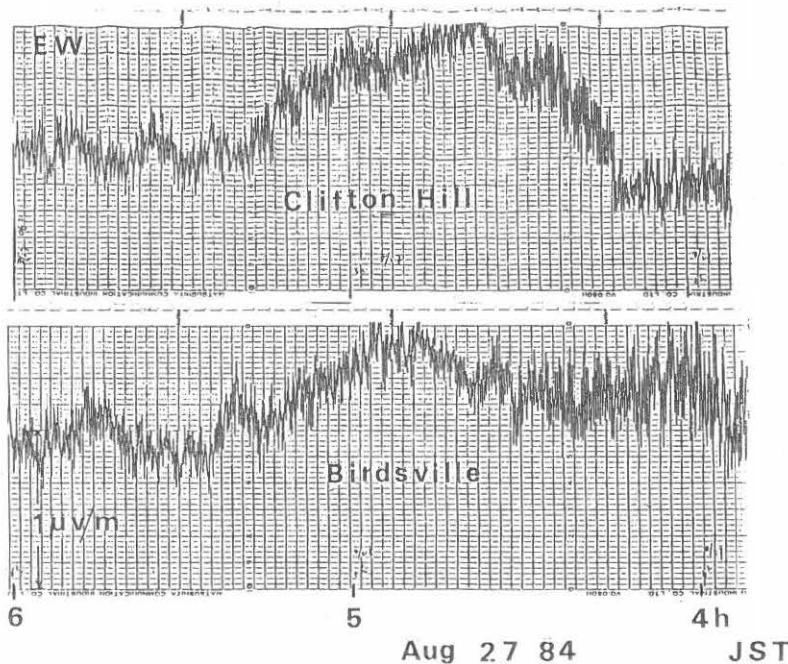


Fig.14 Enhanced EW signals simultaneously observed at Birdsville and Clifton Hill.

5. Appendix

The principle of the digital filter (so-called series-switched filter) performance is indicated in Fig.A-1, as follows (Harden, 1967).

(1) Input sinusoidal signals centred at f_{in} are sampled by the rotary switch revolving at the frequency f_{ck1} . f_{in} and f_{ck1} are chosen to be correlated as

$$f_{in} = f_{ck1} / n$$

,where n is the number of the segments of rotary switch (i.e. the number of the R-C networks).

So, an input sine wave is converted to the (n) -series step-shaped signals on each channel of the R-C networks. Then, the stepped signals are sampled by the (output-side) rotary switch revolving at f_{ck2} , so that one period of the input signals ($1/f_{in}$, sec) is modified as $(1/f_{in}) \times (f_{ck1}/f_{ck2})$, which corresponds to the frequency of output signals : $f_{out} = f_{in} \times (f_{ck1}/f_{ck2})$. The ratio of (f_{ck1}/f_{ck2}) is usually

chosen to be an integer (k). If $k \neq 1$, the input signals are frequency converted to be one k -th.

(2) The bandwidth ($2\Delta f$) of the output signals is independent of all the frequencies (f_{in} , f_{out} , f_{ck1} and f_{ck2}) and is given by

$$\Delta f = 1 / (2\pi nCR) .$$

(3) Noises generated in the filter are proportional to the first sampling (clock) frequency (f_{ck1}) and the resistance value (R).

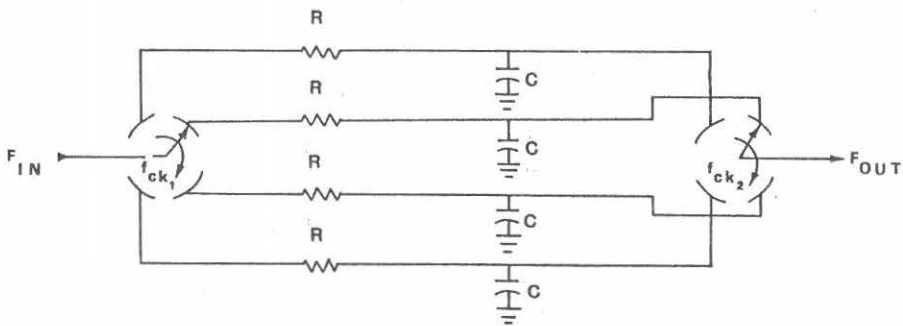


Fig.A-1 Performance principle of the series-switched digital filter in which both the input (f_{in}) and output (f_{out}) signals are sampled by both the rotary switches revolving at frequencies f_{ck1} and f_{ck2} .

The adopted digital filter consists of a pair of 8 channel CMOS analog multiplexers and 8 channel R-C networks connecting the multiplexers. Fig.A-2 illustrates the performance of the digital filter where $f_{ck1}/f_{in} = n = 8$, $f_{ck1}/f_{ck2} = k = 8$, $C = 2.2 \mu F$ and $R = 1 k\Omega$. So, the input signal frequencies of $5.725 \text{ kHz} \pm 10 \text{ Hz}$ are converted down to $715.625 \pm 10 \text{ Hz}$. The frequency converted signals go to the digital filter bank ($n = 8$, $k = 4$, $C = 2.2 \mu F$ and $R = 51 k\Omega$) whose configuration is shown in Fig.A-3. Since the 9 clock frequencies (f_{ck1}) are disposed at an interval of $\pm 4 \text{ Hz}$ centred at 5.725 kHz in the 9 channel digital filters of the filter bank, the input signals ($715.625 \pm 10 \text{ Hz}$) are divided into 9 channel narrow-banded components which are identical to the 9 central frequencies ($715.625 \text{ Hz}, \pm 0.5, \pm 1.0, \pm 1.5$ and $\pm 2.0 \text{ Hz}$) with each bandwidth of 0.4 Hz , corresponding to the antenna input signals at $85.725 \text{ kHz}, \pm 0.5, \pm 1.0, \pm 1.5$ and $\pm 2.0 \text{ Hz}$ with each bandwidth of 0.4 Hz .

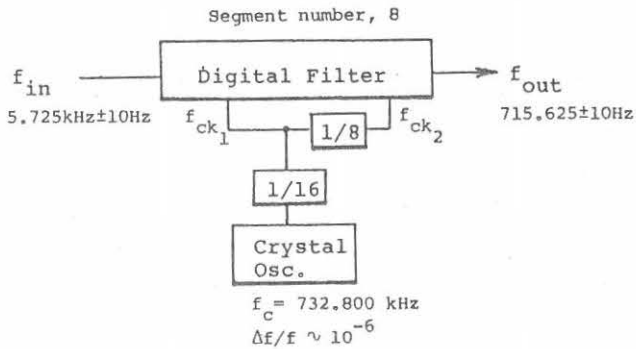


Fig.A-2 Performance of the digital filter.

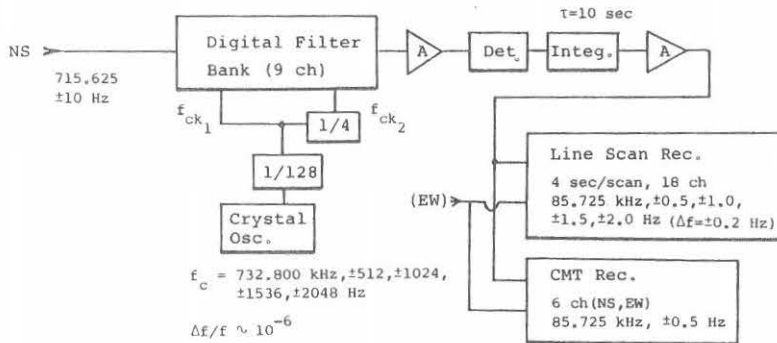


Fig.A-3 Performance of the 9 ch digital filter bank.

On the other hand, noises generated in the digital filter are in direct proportion to the clock frequency (f_{ck1}) and in inverse proportion to the bandwidth (B). If the VLF input signals (5.725 kHz \pm 10 Hz) are supplied not through the digital filter but directly to the 9 channel digital filters of the filter bank (in this case, $f_{ck1} = 8 \times 5.725$ kHz, $B = 0.4$ Hz), noises generated in each of the corresponding 9 channel filters increase by ~ 17 dB as compared with noises in the adopted system (the digital filter, $f_{ck1} = 8 \times 5.725$ kHz, $B = 20$ Hz; each of the 9 channel filters, $f_{ck1} = 5.725$ kHz, $B = 0.4$ Hz). Hence, the adopted digital filter performs not only to convert the input signal frequency but also to reduce the generation of noises.

Acknowledgements

We wish to express our sincere thanks to Drs. K.Lynn and D.Fyfe of the Defence Research Center, Salisbury, S.A., Australia for their continuous cooperation in our scientific survey of 1983-1984 in Australia. Thanks are also due to Mr. R.Goad, Birdsville district police officer, for his various offices during the 1983-1984 observations, in particular his generous approval of the use of observing sites. Simultaneous observations at Birdsville and Clifton Hill were possible due to Mr. G.Wilson's approving his property in Clifton Hill Homestead to be used for our observations. This scientific survey was supported by a Grant-in-Aid for Overseas Scientific Survey from the Ministry of Education of Japan.

References

- Chilton C.J., F.K.Steele and R.B.Norton, VLF phase observations of solar flare ionization in the D region of the ionosphere, *J.Geophys.Res.*, 68, 5421-5435 (1963).
- Doherty R., Oblique incidence pulse measurements at 100 kc/s, in 'Propagation of the radio waves at frequencies below 300 kc/s', 133-148, Pergamon Press (1964).
- Harden W.R., Digital filter with IC's boost Q without inductors, *Electronics*, 40, 91-100 (1967).
- Hayakawa M., Y.Tanaka, T.Okada, J.Ohtsu and A.Iwai, Conjugate measurements of LF, VLF, ELF and ULF waves at Moshiri and Birdsville, *STE Res.*, Japan 7, 12-16 (1983).
- Helliwell R.A. and J.P.Katsufakis, Controlled wave-particle interaction experiments, Upper Atmosphere Research in Antarctica, Antarctic Research Series 29, A.G.U. (1978).
- McNeill F.A. and M.K.Andrews, Quiet-time characteristics of middle-latitude whistler-mode signals during an 8-yr period, *J.Atmos.Terr.Phys.*, 37, 531-542 (1975).